OXFORD

BJS Open, 2024, zrae108
https://doi.org/10.1093/bjsopen/zrae108
Original Article

Role of the serosa in intestinal anastomotic healing: insights from in-depth histological analysis of human and murine anastomoses

Marie-Christin Weber[1,*], Zoé Clees[1], Annalisa Buck[1,2], Adrian Fischer[3], Marcella Steffani[1], Dirk Wilhelm[1], Marc Martignoni[1], Helmut Friess[1], Yuval Rinkevich[3] and Philipp-Alexander Neumann[1,2]

[1]Department of Surgery, Technical University of Munich, TUM School of Medicine and Health, Munich, Germany
[2]Institute for Advanced Study, Technical University of Munich, Munich, Germany
[3]Institute of Regenerative Biology and Medicine, Helmholtz Munich, Munich, Germany

*Correspondence to: Marie-Christin Weber, Department of Surgery, Klinikum rechts der Isar, Technical University of Munich, Ismaninger Str. 22, 81675 München, Germany (e-mail: marie-christin.weber@tum.de)

Abstract

Background: Anastomotic leakage following colorectal surgery remains a significant complication despite advances in surgical techniques. Recent findings on serosal injury repair in coelomic cavities, such as the peritoneum, challenge the current understanding of the cellular origins and mechanisms underlying intestinal anastomotic healing. Understanding the contribution of each layer of the intestinal wall during anastomotic healing is needed to find new therapeutic strategies to prevent anastomotic leakage. The aim of this experimental study was to investigate the role of the serosal layer of the intestinal wall in anastomotic healing.

Materials and methods: Comprehensive histologic analysis of human and murine anastomoses was performed to elucidate histologic changes in the different intestinal layers during anastomotic healing. *In vivo* staining of the extracellular matrix (ECM) in the serosal layer was performed using a fluorophore-conjugated *N*-hydroxysuccinimide-ester before anastomosis surgery in a murine model.

Results: Histological examination of both human and murine anastomoses revealed that closure of the serosal layer occurred first during the healing process. *In vivo* serosal ECM staining demonstrated that a significant portion of the newly formed ECM within the anastomosis was indeed deposited onto the serosal layer. Furthermore, mesenchymal cells within the anastomotic scar were positive for mesothelial cell markers, podoplanin and Wilms tumour protein.

Conclusions: In this experimental study, the results suggest that serosal scar formation is an important mechanism for anastomotic integrity in intestinal anastomoses. Mesothelial cells may significantly contribute to scar formation during anastomotic healing through epithelial-to-mesenchymal transition, potentially suggesting a novel therapeutic target to prevent anastomotic leakage by enhancing physiological healing processes.

Introduction

Anastomotic leakage (AL) after colorectal surgery remains a significant complication. It can lead to short-term morbidity and mortality, increases the risk of local recurrence and decreases disease-free and cancer-specific survival in patients with colorectal cancer[1,2]. Although some risk factors for AL have been elucidated so far, the exact underlying pathological mechanisms are still unclear[3]. Previous research has identified specific strains of collagenase-producing gut bacteria that are associated with AL. This has led to multiple clinical trials on perioperative selective antibiotic decontamination of the gastrointestinal tract before colorectal surgery[4]. Despite this knowledge and use of selective antibiotic decontamination with or without defunctioning ileostomy in clinical practice, AL rates are still unacceptably high[2].

Although recent work has furthered our understanding of the pathophysiological mechanisms during AL, particularly with regards to microbial factors, the physiology of the anastomotic healing process itself remains largely unclear[5–8]. The cellular healing mechanisms of intestinal anastomoses have previously been compared to dermal wound healing despite obvious anatomical differences. The exact cellular and humoral processes of intestinal anastomotic healing have not yet been described. In particular, the origin of fibroblasts and extracellular matrix (ECM)-producing mesenchymal cells within the anastomotic scar remains unknown[8]. The contribution of each individual layer of the intestinal wall (mucosa, submucosa, muscularis and serosa) to the anastomotic healing process remains to be elucidated. There is no clinically established preventative strategy for colorectal AL that supports the healing process itself rather than targeting potential risk factors for AL[9].

In recent years, new insights into healing processes within coelomic cavities such as the peritoneum have emerged[10]. Cell types and general wound-healing mechanisms not previously considered in the healing process of intestinal anastomoses are now being considered in research on the pathophysiology of

Received: June 21, 2024. **Accepted:** July 27, 2024

peritoneal adhesion formation. For example, mesothelial cells, the epithelial cells of the serosal layer of the intestine, and primary peritoneal macrophages have been described as two major cell types involved in peritoneal adhesion formation after abdominal surgery[11,12]. Local activation of mesothelial cells, their proliferation and transition from an epithelial cell type to a mesenchymal cell type (epithelial-to-mesenchymal transition, EMT), followed by ECM deposition and scar formation is now considered to be a major driver of postoperative peritoneal adhesion formation[10,13]. Healing of serosal surfaces within the abdominal wall, in contrast to dermal wound healing, is not only a local process by centripetal migration of mesenchymal cells within the wound, as free-floating mesothelial cells can also be recruited to the injured site[14]. Scar formation depends on pre-made organ ECM that transfers to sites of repair following major injury. As opposed to *de-novo* deposition of new ECM, transfer of pre-made organ ECM is a fundamentally different mechanism to accrual ECM on site, shown to occur in both skin scars and in surgical adhesions in mice[15–18].

The extent that cellular and ECM accrual mechanisms of serosal surface injury repair can be transferred to transmural injury repair, such as intestinal anastomotic healing, has not been investigated yet[8]. The hypothesis is that serosal healing processes contribute not only to the healing of serosal defects but also to the healing of transmural wounds such as intestinal anastomoses. The aim of this study was to investigate serosal involvement in intestinal anastomotic healing by in-depth histological analysis of human and murine intestinal anastomoses.

Methods

Patient samples

Histological samples from human anastomoses were obtained from patients undergoing reoperation and resection of an existing intestinal anastomosis for a reason other than anastomotic leak at the Department of Surgery, Klinikum rechts der Isar, Technical University of Munich or via the Biobank of the Institute of Pathology, Klinikum rechts der Isar, Technical University of Munich (MTBIO) as approved by the Ethics Committee of the Klinikum rechts der Isar, Technical University of Munich (95/22 S-KK; 651/21 S-NP). Informed consent was obtained from patients prior to participation in the study and the biobank. All consecutive samples of resected anastomoses with intact anastomotic healing within a study period of 1 year that were available and for which patient consent was available were included in this study.

Murine intestinal anastomosis model

The animal model for the study of colorectal anastomotic healing was performed as previously described[19,20]. All animal experiments were approved by the Animal Welfare Committee of the Government of Upper Bavaria (No. 55.2-2532.Vet_02-17-203). Murine *in vivo* experiments are reported according to the ARRIVE guidelines. All murine experiments were performed with 9- to 11-week-old female wild-type BALB/c mice. Mice were purchased from Charles River (Sulzfeld, Germany). Mice were housed in the local pathogen-free animal facility under standardized housing conditions, including a 12-hour light/dark cycle at 22°C, 45–60% humidity, and free access to water and standard chow. Environmental enrichment was ensured by providing a nest box, nesting material and scattered food in the bedding. Mice were scored daily for weight, appearance of the fur, behaviour, posture and pain upon abdominal palpation. Colorectal anastomosis surgery was performed as described in the following paragraph. Evaluation time points were postoperative days (POD) 3, 7, 14 and 21. A total of 24 mice were included in the experiment, with six mice being evaluated per time point.

Surgery was performed under general anaesthesia with isoflurane (CP Pharma, Burgdorf, Germany). For perioperative pain management, meloxicam (Boehringer Ingelheim, Ingelheim, Germany) and buprenorphine (Indivior, Berkshire, UK) were administered subcutaneously. Throughout surgery, the body temperature was maintained at 37°C using a heated surgical platform. Prior to anastomosis formation, the serosal ECM was labelled with Alexa Fluor (AF) 568 NHS (succinimidyl) ester (ThermoFisher, Waltham, USA). To do so, 10 µl of the stain was applied on a filter paper covering the descending colon at a concentration of 2.5 mg/ml in reaction buffer (sodium bicarbonate buffer, pH 9; *Fig. 4a*)[21]. The filter paper was removed after 2 min. Colorectal anastomosis surgery was then performed using a microsurgical technique with an operating microscope (Carl Zeiss Meditec, Oberkochen, Germany), following our previously established protocol[19]. In brief, after laparotomy, the colon was exposed and transected below the left kidney to avoid vascular compromise. Subsequently, an end-to-end anastomosis was created using 12–13 single stiches (Ethilon, BV-2, USP 9-0, #2809; Ethicon, Norderstedt, Germany; *Fig. 4b*). The peritoneum and abdominal wall were then closed using the continuous suture technique (Prolene, P3, USP 6-0, #8695H; Ethicon, Norderstedt, Germany).

Histology

Longitudinal transmural sections of formalin-fixed, paraffin-embedded (FFPE) histological samples from human and murine anastomoses were used for histological staining as described below with a section thickness of 3.5 µm for human anastomoses and 2.5 µm for murine anastomoses.

Histological sections were stained with Masson's trichrome with Aniline Blue (Morphisto, Offenbach am Main, Germany) according to the manufacturer's protocol. Stained slides were scanned at 400× magnification using a digital pathology scanner (Aperio AT2, Leica Biosystems, Wetzlar, Germany). The pathology slide-viewing software Aperio ImageScope (Leica Biosystems, Wetzlar, Germany) was used for visualization of scanned histological images.

Histomorphometry

Using Masson's trichrome staining with Aniline Blue, the ECM molecules are stained blue. To assess the proportionate ECM fraction within the anastomotic scar area, the blue area was defined using the colour threshold method in FIJI/ImageJ[22]. The proportionate ECM fraction was then defined as relative to the total tissue area as previously described[23]. The length of the serosal scar and the length of the muscularis gap were measured horizontally along the anastomosis as shown in *Fig. 3d*.

Immunofluorescence

For immunofluorescence staining, histological sections of FFPE blocks were rehydrated and deparaffinized using Roticlear (Carl Roth GmbH, Karlsruhe, Germany), followed by a graded ethanol series. Heat-mediated antigen retrieval was performed with citrate buffer (pH 6) followed by quenching with 50 mM NH_4Cl for 20 min. Samples were permeabilized with 0.25% Triton X-100 in phosphate-buffered serum (PBS) and antigen block was performed with 2% bovine serum albumin (BSA). Samples were

subsequently stained with primary antibodies against type I collagen (COL1; ab88147 (Abcam, Cambridge, UK), 1:100), fibronectin (FN1; ab2413 (Abcam, Cambridge, UK), 1:200), podoplanin (PDPN; murine samples: ab11936 (Abcam, Cambridge, UK), 1:200; human samples: 337001 (Biolegend, San Diego, USA), 1:200), type III collagen (COL3; ab7778 (Abcam, Cambridge, UK), 1:200), alpha smooth muscle actin (αSMA; ab7817 (Abcam, Cambridge, UK), 1:200) and Wilms tumour protein (WT1; ab89901 (Abcam, Cambridge, UK), 1:200) overnight at 4°C. Secondary antibodies (ab150077, AF488 (Abcam, Cambridge, UK); A11005, AF594; A78961, AF594; A21110, AF488 (all Invitrogen, Waltham, USA) and DAPI were incubated for 1 h at room temperature. Slides were mounted with Fluoroshield (Sigma-Aldrich, St. Louis, USA) and imaged with the Zeiss Axio Observer Z1 microscope (Carl Zeiss AG, Oberkochen, Germany).

Gene expression analysis

The mRNA was isolated from murine anastomoses and control colon using the Qiagen RNeasy Mini Kit (Qiagen, Hilden, Germany) according to the manufacturer's instructions. For first strand cDNA synthesis, the Qiagen RT^2 First Strand kit (Qiagen, Hilden, Germany) was used. Quantitative PCR was then performed on the LightCycler 480 platform (Roche, Basel, Switzerland) using KAPA SYBR Fast DNA polymerase (Roche, Basel, Switzerland). The following primers were used: *Hprt*: forward 5′-TCAGTCAACGGGGGACATAAA-3′, reverse 5′-GGGGC TGTACTGCTTAACCAG-3′; *Col1a1*: forward 5′-TAAGGGTCCCCAA TGGTGAGA-3′, reverse 5′-GGGTCCCTCGACTCCTACAT-3′; *Lox*: forward 5′-GATGCGCTGCGGAAGAAAAC-3′, reverse 5′-GTACCCT GTGGTCATAGTCTCT-3′; *Fn1*: forward 5′-CCCTATCTCTGATACC GTTGTCC-3′, reverse 5′-TGCCGCAACTACTGTGATTCGG-3′; *Wt1*: forward 5′-GGTTTTCTCGCTCAGACCAGCT-3′, reverse 5′-ATGA GTCCTGGTGTGGGTCTTC -3′; *Snai1*: forward 5′-TGTCTGCACGA CCTGTGGAAAG-3′, reverse 5′-CTTCACATCCGAGTGGGTTTG G-3′; *Snai2*: forward 5′-TCTGTGGCAAGGCTTTCTCCAG-3′, reverse 5′-TGCAGATGTGCCCTCAGGTTTG-3′. Relative mRNA expression is represented as relative expression ($2^{-\Delta CT}$) normalized to *Hprt*.

Statistical analysis and data visualization

GraphPad Prism (version 10.1.0; GraphPad Software, San Diego, USA) was used for data visualization and statistical analysis. Statistical differences were calculated using the one-way ANOVA with Tukey's multiple comparison test. $P < 0.05$ was considered statistically significant. Figures were created using Adobe Illustrator (Adobe Inc., San José, USA) and Adobe Lightroom was used to enhance contrast for better visualization of histologic images in the figures.

Results

Intact anastomoses from seven different patients were included in the study, two from the early postoperative phase (POD 7 and 9) and five from the late postoperative phase (1.5–16 years after surgery). A total of 24 mice were included in the experiment, with six mice being evaluated per time point.

Early postoperative human intestinal anastomoses are characterized by profound serosal extracellular matrix accumulation

Two patient cases in which a newly formed intestinal anastomosis was resected early following surgery for reasons other than AL were analysed histologically.

Anastomosis 1 is a double-layered hand-sewn jejuno-jejunal anastomosis that was resected 7 days following surgery due to bleeding at the anastomosis. Histologically, a profound thickening of the serosal layer with accumulation of ECM was observed in the Masson's trichrome–stained section (*Fig. 1a*). The muscularis, submucosal and mucosal layers are not closed, and the anastomosis seems to be primarily sealed at the serosal layer, with clear signs of ECM deposition at that site. The same findings are present in histological section from different regions of the anastomosis as shown in *Fig. S2a*. Immunohistologically, ECM deposition within the serosal layer was confirmed and large amounts of type I collagen (COL1) and fibronectin (FN1) were observed within the serosal scar (*Fig. 1b*). A schematic overview of the histological findings is shown in *Fig. 1c*.

Anastomosis 2 is an ileocolonic anastomosis that was resected on POD 9 due to an incidental histological cancer finding in the initial surgical specimen from an ileocaecal resection for acute small bowel obstruction. Similar to anastomosis 1, the serosal layer is the only closed layer within the anastomosis, and again, no tissue bridges have formed between the muscularis, submucosal and mucosal layers of the joined bowel ends within the anastomosis (*Fig. S2b*). To demonstrate the structure of the native intestinal wall, histological images of a small bowel segment are shown in *Fig. S2c*.

Muscularis layer replaced by fibrotic scar in human anastomoses

Intestinal anastomoses from five patients were resected in the late postoperative period (1.5–16 years after surgery) and were analysed histologically.

Anastomosis 3 is a hand-sewn side-to-side double-layered ileal–ileal anastomosis that was resected 1.5 years after ileostomy reversal in a patient with Crohn's disease (*Table S2*). Sections from two different areas of the anastomosis are shown (*Fig. 2a*). The muscularis layer is not closed within the anastomosis but the wound is characterized by a fibrotic scar (marked by the asterisk in the figure) on which the mucosal layer has regenerated. The fibrotic scar appears to originate from the serosal layer of the intestinal wall.

Anastomosis 4 is an end-to-end circular stapled colorectal anastomosis resected 2 years after the index surgery. Again, the muscularis layer is not closed and the wound area is filled with fibrotic scar tissue with marked ECM deposition on the adventitial side of the intestinal wall (*Fig. 2b*). Not only is the muscularis layer disrupted by scar tissue within the anastomotic area, but portions of the muscularis are remodelled and replaced by fibrosis around the anastomotic area (indicated by '**##**').

Anastomosis 5 is a hand-sewn, side-to-side double-layered ileal–ileal anastomosis that was resected 3 years after ileostomy reversal due to adhesive acute bowel obstruction distal of the anastomosis. Similar to anastomoses 3 and 4, the muscularis layer has not been regenerated and the scar is characterized by fibrotic tissue, but isolated groups of smooth muscle cells are present within the scar tissue (*Fig. 2c*).

Anastomosis 6 is another ileal–ileal anastomosis from a patient with Crohn's disease that was resected 7 years following index surgery. Within the anastomotic area, the muscularis layer is not closed and the gap is filled by a fibrotic scar. A profound thickening of the serosal layer around the scar area can be observed. A deep lymphocytic ulceration (indicated by ** in *Fig. 2d*) associated with the underlying Crohn's disease is present within the anastomotic scar.

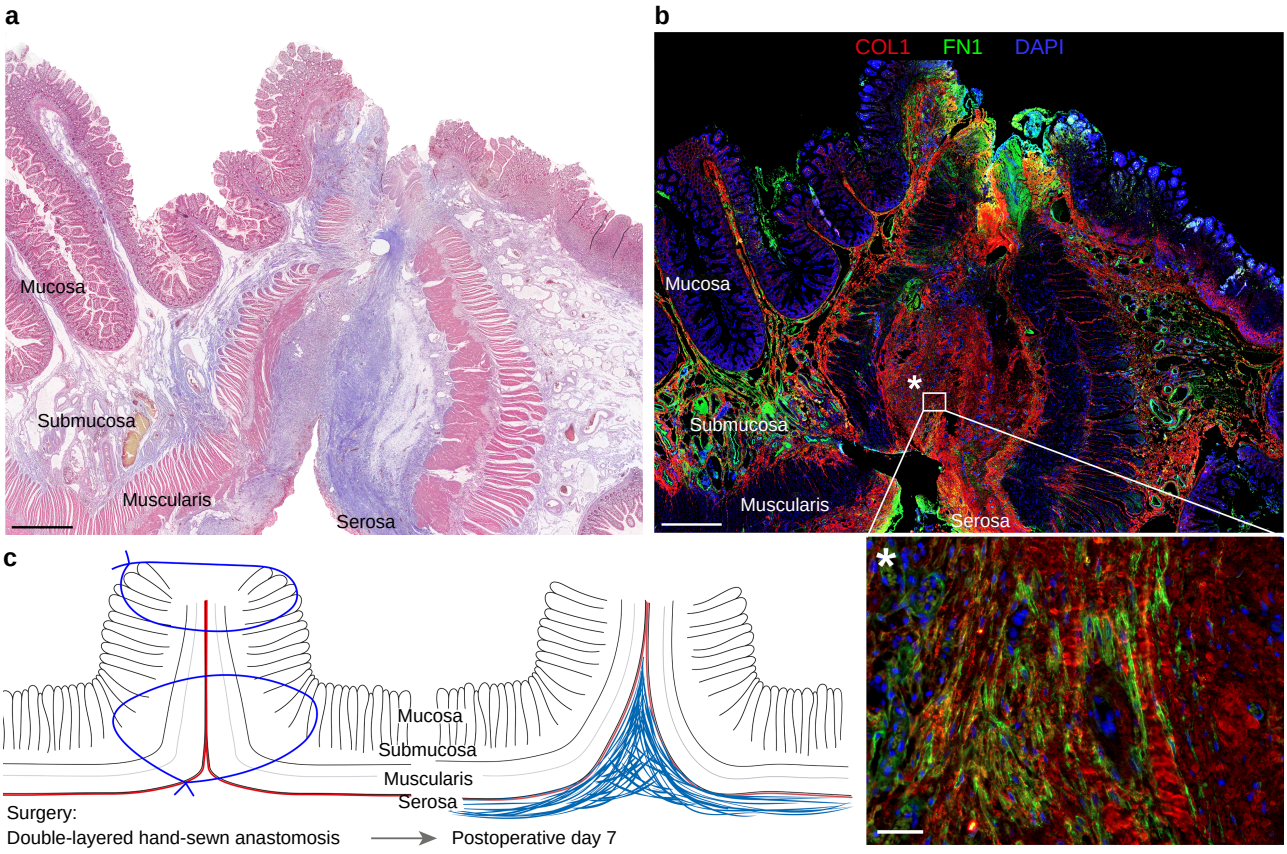

Fig. 1 Histological evaluation of early postoperative human intestinal anastomosis

a Overview scan of Masson's trichrome-stained histologic section of human anastomosis (double-layered inverted hand-sewn jejuno-jejunal anastomosis) at postoperative day (POD) 7 shows serosal scar formation sealing the anastomosis. The mucosal, submucosal and muscularis layers are not closed yet. Scale bar = 1000 µm, 400× magnification. **b** Immunofluorescence staining for fibronectin (FN1) and type I collagen (COL1) of the same human anastomosis as in **a** shows pronounced serosal scarring and accumulation of the extracellular matrix (ECM) proteins fibronectin and type I collagen. Scale bar = 1000 µm, 100× magnification (top), scale bar = 50 µm, 200× magnification (bottom). **c** Schematic representation of serosal scar formation of a double-layered inverted hand-sewn anastomosis on the day of surgery and on POD 7.

Anastomosis 7 is an ileocolonic anastomosis resected 16 years after ileocaecal resection in a patient with Crohn's disease due to a recurrent stricture aboral of the initial anastomosis (*Fig. 2e*). The exact surgical technique could not be derived from the patient records, but a hand-sewn double-layered anastomotic technique appeared to be the most likely technique used. The muscularis layer had not closed, but the anastomosis was sealed with fibrotic scar tissue on the serosal side of the anastomosis. It should be noted that the mucosal layer was intact in the surgical specimen but missing (blue line) in the histological section due to technical factors.

End-to-end partially everted murine anastomoses are sealed by extracellular matrix deposition on the serosal side of the intestinal wall

To further analyse the early postoperative events of serosal scar formation during intestinal anastomotic healing, a murine model of colorectal anastomosis and histologically analysed longitudinal sections of the anastomoses at POD 3, 7, 14 and 21 were used. In contrast to human anastomoses, anastomosis in the murine model was formed as an end-to-end anastomosis and closed with single sutures. As the murine colon everts after transection, the mucosal layer is naturally partially everted within the anastomosis (*Fig. 3a*, POD 3; *Fig. 4b*). Although at POD 3 there was little to no accumulation of ECM within the anastomotic area, at POD 7 the anastomosis was already sealed with a layer of ECM derived from the serosal side of the intestinal wall (*Fig. 3a*). Between POD 7 and POD 14–21 little change within the anastomotic structure was observed. As such, the mean(s.d.) proportionate ECM fraction within the anastomotic area was 10.0(3.1)% at POD 3, 23.1(23.1)% at POD 7 and 25.7(9.5)% at POD 21 (*Fig. 3b*). The mean(s.d.) length of the serosal scar increased after surgery from 2.7(0.7) mm at POD 3 to 5.5(1.2) mm at POD 21 ($P < 0.0001$; *Fig. 3c*). Similar to observations in the human anastomoses, the muscularis layer did not regenerate during the healing process and the muscularis gap between the adjacent bowel ends even increased during the postoperative period (0.7(0.2) mm at POD 3 and 1.2(0.1) mm at POD 21, $P = 0.003$; *Fig. 3d*). At POD 7, the mucosal layer was in a state of regeneration in most samples. The formation of a single epithelial cell layer of mucosal progenitor cells on the ECM-rich scar tissue preceded the regeneration of fully developed mucosal crypts (*Fig. S3a–c*). Like the mucosal layer, the lamina muscularis mucosa also did not regenerate during the healing process (*Fig. S3d*).

Newly formed extracellular matrix is deposited on the serosal layer in murine anastomoses

To verify that the serosal scar was indeed formed on top of the mesothelial lining of the serosa and not between the muscularis

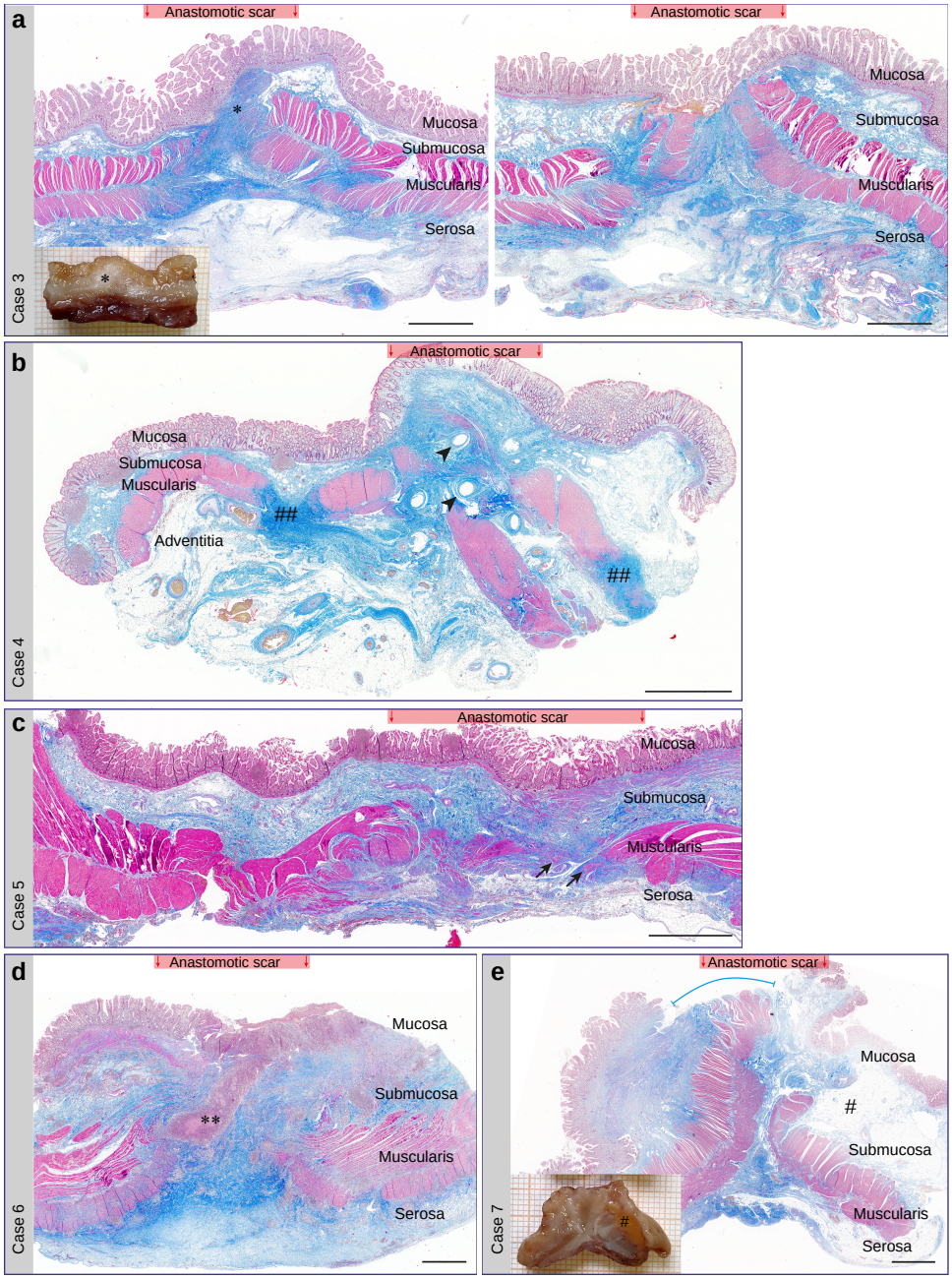

Fig. 2 Histological evaluation of late postoperative human anastomoses

a–e Overview scans of Masson's trichrome–stained sections of human anastomoses from late postoperative periods. Data on patient cases and type of anastomosis are described in *Table S2*. Scale bars = 2000 µm, 400× magnification. **a + e** Additional photograph of formalin-fixed tissue prior to paraffin embedding for further histological slide preparation. Additional markings in histologic images: **a** *submucosal scar formation within the anastomotic scar area. Left and right histological images are from different regions of the same anastomosis. **b** ##fibrosis of the muscularis layer around the anastomotic scar. Arrow heads indicate stapler holes. **c** Arrows indicate isolated groups of smooth muscle cells within anastomotic scars. **d** **ulceration at anastomotic site due to underlying Crohn's disease. **e** #submucosal fat tissue accumulation due to underlying Crohn's disease. The line marks the partially missing mucosa layer in histological section; the mucosal layer was closed above the anastomosis in the surgical specimen.

and serosa, we stained the serosal ECM including its basement membrane with Alexa Fluor 568 NHS ester before performing the colorectal anastomosis (*Fig. 4a,b*). Immunofluorescence counterstaining showed that most PDPN-positive cells within the margins of the anastomosis were located on top of the stained serosa at POD 7 (*Fig. 4c*). In addition, while some FN1$^+$ ECM fibres were present below the stained serosa, newly formed COL3 was only present on top of the serosa (*Fig. 4d,e*). A similar pattern was observed at POD 14 and 21 (*Fig. S4*).

Mesenchymal cells within anastomotic scar express mesothelial cell markers

As it is known that mesothelial cells within the serosal layer can undergo EMT during peritoneal healing processes such as adhesion formation, human and murine anastomoses were stained for the EMT marker αSMA and the mesothelial cell-specific EMT marker WT1[13]. Mesenchymal cells within the serosal scar of human anastomoses (Cases 1 and 2) stained positive for αSMA and PDPN/WT1 (*Fig. 5a,b*, images show staining

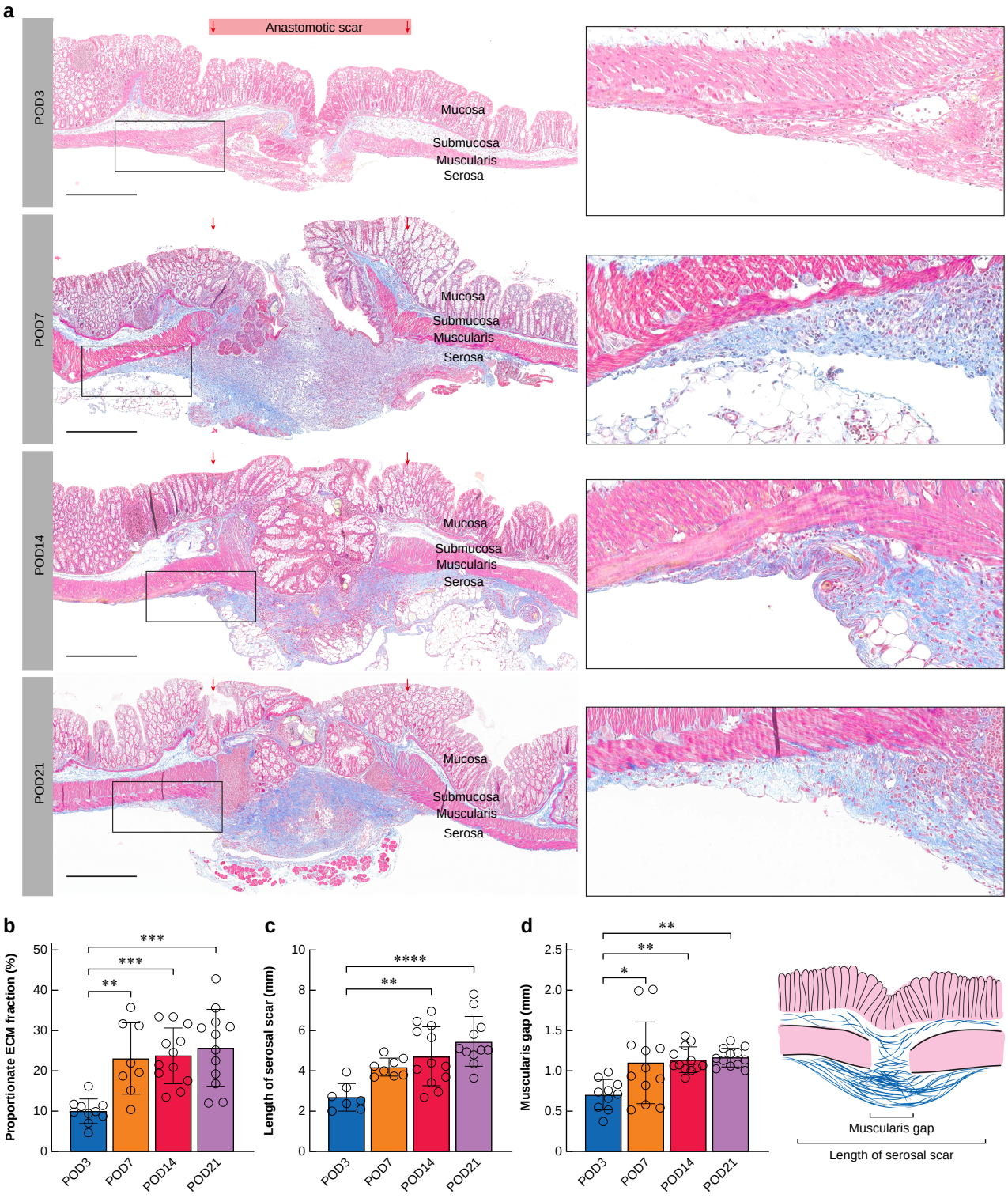

Fig. 3 Histological evaluation of murine intestinal anastomosis

a Overview scans of Masson's trichrome–stained histological sections of murine anastomoses at postoperative day (POD) 3, 7, 14 and 21. Scale bar = 500 µm, 400× magnification. Gradual accumulation of extracellular matrix (ECM) on the serosal side of the anastomosis can be seen from POD 7. **b** Proportional ECM fraction within the anastomotic scar compared to the total tissue area in % for POD 3–21. **c** Length of the serosal scar in mm for POD 3–21. **d** Muscularis gap in mm for POD 3–21. Schematic representation of histomorphometric parameters at the lower left. **b–d** $n = 4–6$ per time point with two technical replicates per sample. One-way ANOVA with Tukey's multiple comparison test, $^{*}P < 0.05$, $^{**}P < 0.01$, $^{***}P < 0.001$, $^{****}P < 0.0001$. Data are mean(s.d.) with dots for individual values.

from Case 1). Similarly, in the murine anastomoses, $WT1^{+}PDPN^{+}$ cells are abundant within the serosal scar (*Fig. 5c*). Interestingly, whereas $WT1^{+}PDPN^{+}$ cells were still round and epithelial-like at the edge of the scar, their phenotype was more spindle cell–like in the centre of the scar tissue, indicating EMT of these cells (*Fig. 5c*, white arrowheads). Gene expression analysis of murine anastomotic tissue revealed a peak in the expression of the ECM molecules *Col1a1* and *Fn1* and the cross-linking enzyme lysyl

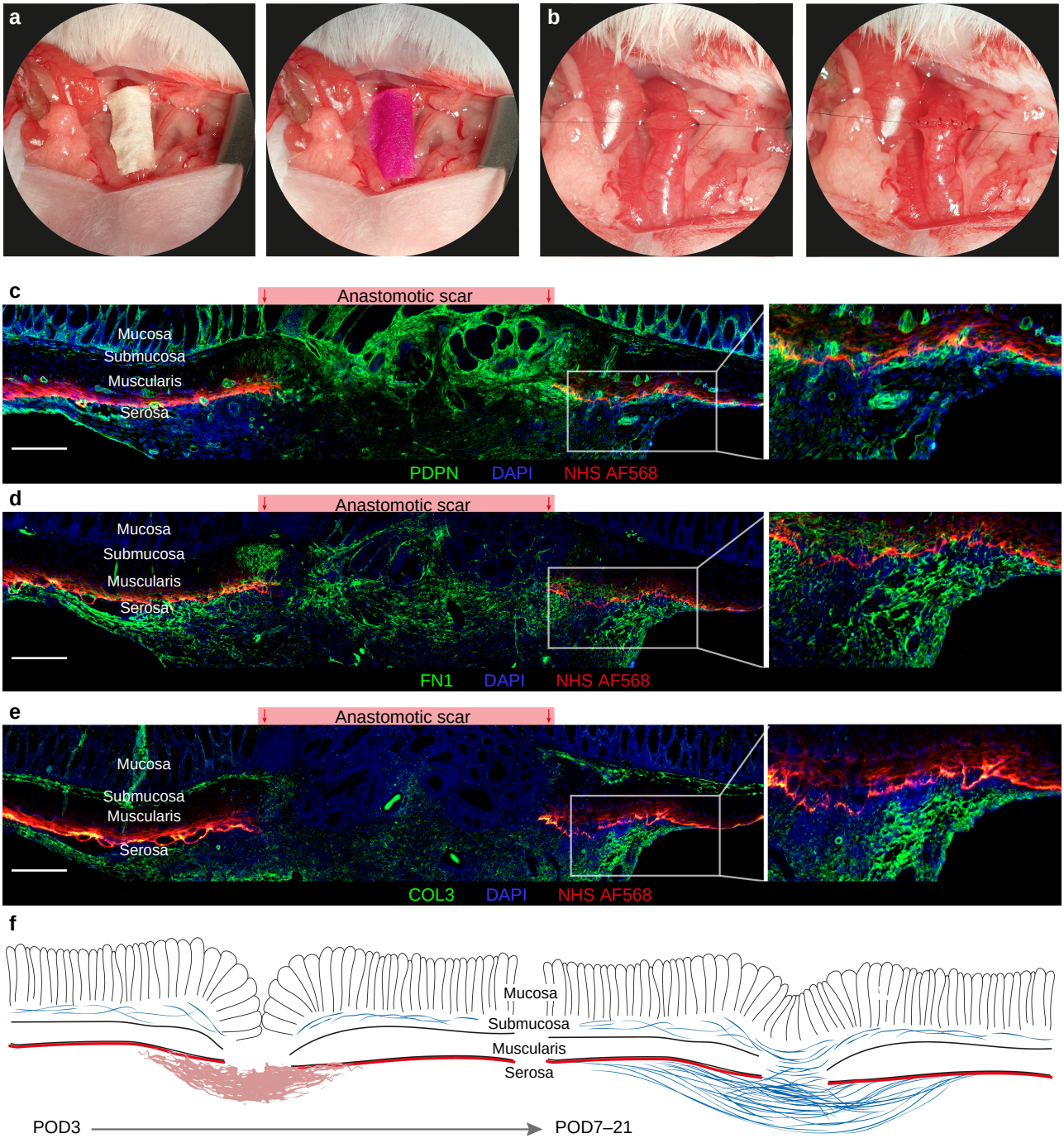

Fig. 4 Serosal scar formation in murine anastomosis model

a + **b** Murine surgery model of colorectal anastomosis, exemplary intraoperative photographs. **a** First, the serosal layer of the descending colon is stained with an Alexa Fluor 568 conjugated *N*-hydroxysuccinimide ester (NHS AF568). **b** The colon is then transected, and two holding sutures are placed at either side of the transected bowel ends. The anastomosis is then closed with single stitches. **c–e** *In vivo* serosal staining with NHS AF568 prior to anastomosis surgery and co-staining with **c** podoplanin (PDPN), **d** fibronectin (FN1) and **e** type 3 collagen (COL3). PDPN-positive cells as well as the extracellular matrix (ECM) proteins FN1 and COL3 are deposited on top of the serosal layer as marked in red by the NHS AF568. Representative images of anastomosis at postoperative day (POD) 7. Scale bar = 200 µm, 100× magnification. $n = 2–3$ for POD 7, 14 and 21. **f** Schematic representation of serosal scar formation in murine anastomoses.

oxidase (*Lox*) at POD 7. Furthermore, the mesothelial cell EMT marker WT1 was significantly upregulated at POD 7 compared to control colon as well as the EMT transcription factors *Snai1* and *Snai2* (*Fig. 5d*).

Discussion

An evidence-based, detailed understanding of the mechanisms underlying anastomotic healing is still lacking, hindering the identification of preventative therapeutic approaches to prevent AL[8]. In particular, the role of each layer of the intestinal wall during the anastomotic healing process, the origin of the mesenchymal cells responsible for ECM deposition and scar formation and the timing of mucosal re-epithelialization and submucosal scar formation have not yet been elucidated.

Because scar formation and deposition of ECM is the crucial step in most healing processes, histological staining for ECM proteins in human anastomoses at different postoperative time

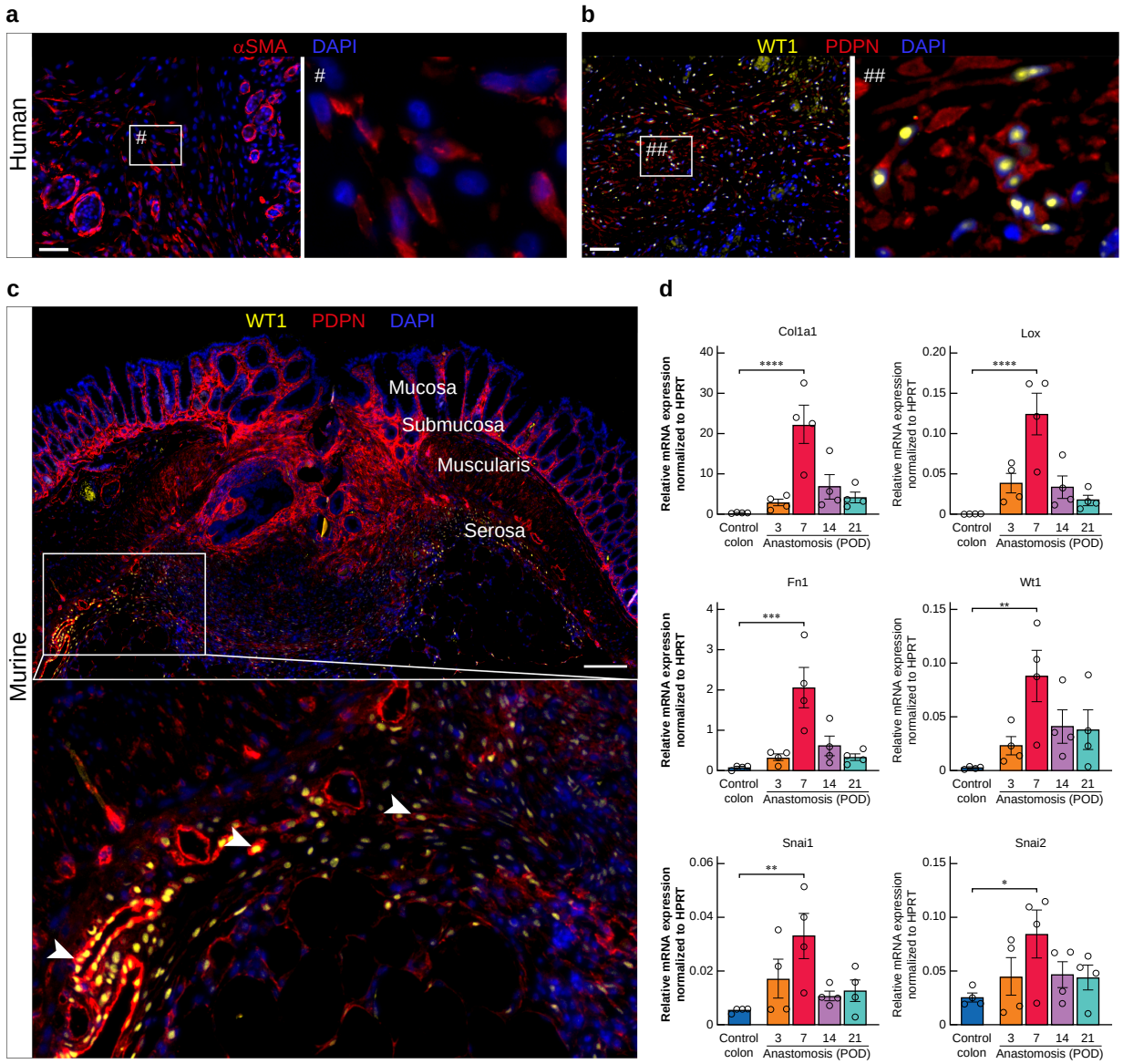

Fig. 5 Cells within the anastomotic serosal scar express mesothelial cell markers

a Immunofluorescence (IF) staining for alpha smooth muscle actin (αSMA) shows αSMA$^+$ cells and microvessels within the serosal scar of human anastomosis at postoperative day (POD) 7. Scale bar = 50 µm, 200× magnification. **b** IF staining for Wilms tumour protein (WT1) and podoplanin (PDPN) showing the presence of WT1$^+$PDPN$^+$ mesothelial cells (MCs) within the anastomotic scar of human anastomosis at POD 7. Scale bar = 50 µm 200× magnification. **c** IF staining for WT1 and PDPN showing the presence of WT1$^+$PDPN$^+$ MCs within the anastomotic scar of murine anastomosis at POD 7. White arrowheads: transition of WT1$^+$PDPN$^+$ cells from epithelial to mesenchymal phenotype within the anastomotic scar. Scale bar = 200 µm, 100× magnification, $n = 3$. **d** Relative gene expression of extracellular matrix-associated proteins (*Col1a1*, *Fn1*, *Lox*), mesothelial cell markers (*Wt1*) and key epithelial-to-mesenchymal transition (EMT) transcription factors (*Snai1*, *Snai2*) within murine anastomosis at POD 3, 7, 14 and 21 compared to murine control colon. $n = 4$ per time point, one-way ANOVA with Tukey's multiple comparison test to control colon, $^*P < 0.05$, $^{**}P < 0.01$, $^{***}P < 0.001$, $^{****}P < 0.0001$. Data are mean(s.e.m.) with dots for individual values.

points were performed to gain an understanding of the histological features of human anastomoses during the early healing phase. The striking feature of the two human anastomoses obtained in the early healing phase was a profound deposition of ECM on the serosal side of the anastomoses. In both anastomoses analysed, the thickened serosal layer was the first layer of the intestinal wall to be completely closed within the anastomoses. The muscularis, submucosal and mucosal layers were not reconnected at POD 7 and 9. Given that the anastomoses were performed using a hand-sewn double-layered inverted technique, which is the standard in our clinic, the findings may be expected. Baskén and Renvall studied colonic anastomoses in rats in the year 1990, demonstrating that formation of granulation tissue on the serosal surfaces within the anastomosis was pronounced in the first postoperative week[24]. When looking at early postoperative anastomoses (Anastomoses 1 and 2), it could be that the serosa was already thickened at the time of surgery (for example due to a local inflammatory reaction or scar tissue from previous operations). Other causes such as the underlying disease (for example Crohn's disease) could contribute to fibrosis of the serosa due to transmural inflammation. Nevertheless, the serosa is the only layer that is completely closed in the anastomosis. The topic of serosal healing and its potential therapeutic availability in the search for preventative strategies for AL has not yet been investigated.

In contrast to the surgical technique used in human patients, anastomoses in the murine model are performed as end-to-end anastomoses and closed with single sutures. Due to the small size of the anastomosis compared to the available suture material and the intrinsic tendency of the colon wall to evert after transection, the mucosa in the murine model is slightly everted so that the serosal layers in the newly formed anastomosis are not opposed. However, despite the technical difference, most of the ECM-rich scar tissue sealing the anastomosis was deposited on the serosal side of the intestinal wall. Only after the anastomosis was sealed with ECM-rich scar tissue would the mucosal layer re-epithelialize into the anastomotic defect (*Fig. S3*).

As one of the cellular origins of mesenchymal cells and fibroblasts during serosal healing processes, mesothelial cells have been identified as responsible for ECM formation after undergoing EMT[11,25,26]. We identified the mesothelial EMT marker WT1 in both human and mouse anastomoses, suggesting the involvement of mesothelial cells in intestinal anastomotic healing (*Fig. S5*).

The data presented in this study support the hypothesis that serosal healing processes and mesothelial cells may contribute not only to the healing of serosal defects but also to the healing of transmural wounds such as intestinal anastomoses; however, further mechanistic studies are needed. Further research is needed to identify the signalling pathways behind serosal scar formation during intestinal anastomotic healing. By not only controlling the factors that contribute to AL but also improving the physiological processes of anastomotic healing, it may be possible in the future to significantly reduce the clinical burden of intestinal AL. A better understanding of the physiology of the anastomotic healing process itself may also help to identify the root causes of AL and thus help to target them to improve outcomes in colorectal surgery.

There are several limitations to this study. A key aspect is that the data are mainly descriptive. The data presented so far cannot prove that mesothelial cell-initiated scarring of the serosa contributes decisively to anastomotic healing and that increased rates of anastomotic leakage would occur without this mechanism. Although not yet mechanistically proven, the descriptive data on human and murine anastomoses presented in this study are highly suggestive, especially in combination with the current literature on serosal healing processes after serosal injury[10,11,13]. Experimentally inhibiting mesenchymal differentiation of mesothelial cells following surgery and lineage-tracing of mesothelial cells *in vivo* would be the next steps to further prove our hypothesis. However, the fact that anastomoses with only unilateral or no serosal involvement heal in most cases certainly also indicates that the presumed mesothelial cell involvement in the anastomotic healing process is only one of the factors contributing to the healing process and that anastomoses can also heal without these cells. Experimental data showing that inhibition of serosal healing increases the risk of anastomotic leakage even in anastomoses with bilateral serosal involvement is still lacking. In addition, other aspects of the healing process such as the fibrotic remodelling of the anastomotic tissue after the enzymatic degradation of the damaged tissue in the initial healing phase should also be investigated.

Funding

M.C.W. was supported by the Else Kröner Memorial Fellowship funded by the Else Kröner-Fresenius-Stiftung (2023_EKMS.13). Y.R. was supported by the European Research Council (ERC-CoG 819933), the LEO Foundation grant LF-OC-21-000835, the European Foundation for the Study of Diabetes (EFSD) Anniversary Fund Programme 2021, and the Deutsche Forschungsgemeinschaft SFB TRR 359 (PILOT).

Disclosure

The authors declare no conflicting interests regarding this study.

Supplementary material

Supplementary material is available at *BJS Open* online.

Data availability

All data supporting the findings of this study are available within the paper and its Supplementary material. High-quality histological images can be obtained from the corresponding author upon reasonable request.

Author contributions

Marie-Christin Weber (Conceptualization, Data curation, Formal analysis, Funding acquisition, Methodology, Validation, Visualization, Writing—original draft, Writing—review & editing), Zoé Clees (Conceptualization, Formal analysis, Investigation, Methodology, Writing—review & editing), Annalisa Buck (Investigation, Writing—review & editing), Adrian Fischer (Conceptualization, Investigation, Methodology, Writing—review & editing), Marcella Steffani (Investigation, Writing—review & editing), Dirk Wilhelm (Resources, Writing—review & editing), Marc Martignoni (Resources, Writing—review & editing), Helmut Friess (Resources, Writing—review & editing), Yuval Rinkevich (Methodology, Writing—review & editing), and Philipp-Alexander Neumann (Conceptualization, Methodology, Supervision, Writing—review & editing)

References

1. Mirnezami A, Mirnezami R, Chandrakumaran K, Sasapu K, Sagar P, Finan P. Increased local recurrence and reduced survival from colorectal cancer following anastomotic leak: systematic review and meta-analysis. *Ann Surg* 2011;**253**:890–899
2. Weber MC, Berlet M, Stoess C, Reischl S, Wilhelm D, Friess H *et al.* A nationwide population-based study on the clinical and economic burden of anastomotic leakage in colorectal surgery. *Langenbecks Arch Surg* 2023;**408**:55
3. Lam A, Fleischer B, Alverdy J. The biology of anastomotic healing—the unknown overwhelms the known. *J Gastrointest Surg* 2020;**24**:2160–2166
4. Shogan BD, Belogortseva N, Luong PM, Zaborin A, Lax S, Bethel C *et al.* Collagen degradation and MMP9 activation by *Enterococcus faecalis* contribute to intestinal anastomotic leak. *Sci Transl Med* 2015;**7**:286ra68
5. Hajjar R, Santos MM, Dagbert F, Richard CS. Current evidence on the relation between gut microbiota and intestinal anastomotic leak in colorectal surgery. *Am J Surg* 2019;**218**:1000–1007
6. Hajjar R, Gonzalez E, Fragoso G, Oliero M, Alaoui AA, Calvé A *et al.* Gut microbiota influence anastomotic healing in colorectal cancer surgery through modulation of mucosal proinflammatory cytokines. *Gut* 2023;**72**:1143–1154

7. Shogan BD, Carlisle EM, Alverdy JC, Umanskiy K. Do we really know why colorectal anastomoses leak? *J Gastrointest Surg* 2013;**17**:1698–1707
8. Rosendorf J, Klicova M, Herrmann I, Anthis A, Cervenkova L, Palek R *et al.* Intestinal anastomotic healing: what do we know about processes behind anastomotic complications. *Front Surg* 2022;**9**:904810
9. Bosmans JW, Jongen AC, Bouvy ND, Derikx JP. Colorectal anastomotic healing: why the biological processes that lead to anastomotic leakage should be revealed prior to conducting intervention studies. *BMC Gastroenterol* 2015;**15**:180
10. Zwicky SN, Stroka D, Zindel J. Sterile injury repair and adhesion formation at serosal surfaces. *Front Immunol* 2021; **12**:684967
11. Tsai JM, Sinha R, Seita J, Fernhoff N, Christ S, Koopmans T *et al.* Surgical adhesions in mice are derived from mesothelial cells and can be targeted by antibodies against mesothelial markers. *Sci Transl Med* 2018;**10**:eaan6735
12. Zindel J, Peiseler M, Hossain M, Deppermann C, Lee WY, Haenni B *et al.* Primordial GATA6 macrophages function as extravascular platelets in sterile injury. *Science* 2021;**371**:eabe0595
13. Fischer A, Koopmans T, Ramesh P, Christ S, Strunz M, Wannemacher J *et al.* Post-surgical adhesions are triggered by calcium-dependent membrane bridges between mesothelial surfaces. *Nat Commun* 2020;**11**:3068
14. Foley-Comer AJ, Herrick SE, Al-Mishlab T, Prêle CM, Laurent GJ, Mutsaers SE. Evidence for incorporation of free-floating mesothelial cells as a mechanism of serosal healing. *J Cell Sci* 2002;**115**:1383–1389
15. Correa-Gallegos D, Jiang D, Christ S, Ramesh P, Ye H, Wannemacher J *et al.* Patch repair of deep wounds by mobilized fascia. *Nature* 2019;**576**:287–292
16. Jiang D, Christ S, Correa-Gallegos D, Ramesh P, Kalgudde Gopal S, Wannemacher J *et al.* Injury triggers fascia fibroblast collective cell migration to drive scar formation through N-cadherin. *Nat Commun* 2020;**11**:5653
17. Wan L, Jiang D, Correa-Gallegos D, Ramesh P, Zhao J, Ye H *et al.* Connexin43 gap junction drives fascia mobilization and repair of deep skin wounds. *Matrix Biol* 2021;**97**:58–71
18. Fischer A, Wannemacher J, Christ S, Koopmans T, Kadri S, Zhao J *et al.* Neutrophils direct preexisting matrix to initiate repair in damaged tissues. *Nat Immunol* 2022;**23**:518–531
19. Miltschitzky JRE, Clees Z, Weber MC, Vieregge V, Walter RL, Friess H *et al.* Intestinal anastomotic healing models during experimental colitis. *Int J Colorectal Dis* 2021;**36**:2247–2259
20. Weber MC, Bauer J, Buck A, Clees Z, Oertel R, Kasajima A *et al.* Perioperative low-dose prednisolone treatment has beneficial effects on postoperative recovery and anastomotic healing in a murine colitis model. *J Crohns Colitis* 2023;**17**:950–959
21. Fischer A, Correa-Gallegos D, Wannemacher J, Christ S, Machens HG, Rinkevich Y. *In vivo* fluorescent labeling and tracking of extracellular matrix. *Nat Protoc* 2023;**18**: 2876–2890
22. Schindelin J, Arganda-Carreras I, Frise E, Kaynig V, Longair M, Pietzsch T *et al.* FIJI: an open-source platform for biological-image analysis. *Nat Methods* 2012;**9**:676–682
23. Weber MC, Schmidt K, Buck A, Kasajima A, Becker S, Li C *et al.* Fractal analysis of extracellular matrix for observer-independent quantification of intestinal fibrosis in Crohn's disease. *Sci Rep* 2024;**14**:3988
24. Braskén P, Renvall S. Local energy metabolism in healing colon anastomosis. An enzyme-histochemical study in rats. *Acta Chir Scand* 1990;**156**:565–570
25. Mutsaers SE. Mesothelial cells: their structure, function and role in serosal repair. *Respirology* 2002;**7**:171–191
26. Mutsaers SE, Birnie K, Lansley S, Herrick SE, Lim CB, Prêle CM. Mesothelial cells in tissue repair and fibrosis. *Front Pharmacol* 2015;**6**:113